https://doi.org/10.1016/j.jmatprotec.2017.10.022

Deformation characteristic and geometrical size effect in continuous manufacturing of cylindrical and variable-thickness flanged microparts

B. Meng[1, 2], M.W. Fu*[,2, 3], S.Q. Shi[2]

[1]School of Mechanical Engineering and Automation, Beihang University, Beijing 100191, P.R. China

[2]Department of Mechanical Engineering, The Hong Kong Polytechnic University, Hung Hom, Kowloon, Hong Kong

[3]PolyU Shenzhen Research Institute, No. 18 Yuexing Road, Nanshan District, Shenzhen, P.R. China

*Corresponding author. Tel: 852-27665527. E-mail address: mmmwfu@polyu.edu.hk

Abstract

The most critical issues in microforming technologies are tailoring the desirable product quality and ensuring the high productivity from application perspective. This is also the case for fabrication of cylindrical micro-pin and flanged micropart with nonuniform thickness. To realize continuous micromanufacturing of the hollow flanged micropart with variable thickness, an efficient progressive microforming method is proposed by using an integrated hole flanging-ironing process. In this process, size effect and its affected deformation behavior and forming quality of the micropart are still not well known and knowing of them well is crucial in forming of the accurate shape and geometry of the microparts, tailoring the needed product properties and assuring the required qualities. This study thus aims at addressing these issues in terms of deformation load, forming kinematics, dimensional accuracy, defect formation and microstructural evolution based on an unequal-thickness

flanged micropart produced by the developed progressive microforming system in which shearing, hole flanging-ironing and blanking operations are realized progressively. The experimental results reveal that the length of the flanged micropart is reduced with the increasing grain size, while both the tapering angle and its scatter present an opposite tendency, which could be explained by the coupled model of free surface roughening and open and closed lubricant pockets. Furthermore, the dimensional accuracy, surface appearance and the defects including curved profile, singularity, wrinkling and irregularity are closely related to the initial material microstructure. Through realization and examination of the developed progressive microforming system and the finished microparts, the progressive hole flanging-ironing process is proven to be promising and efficient for continuous micromanufacturing of micro-scaled hollow products with higher flange and variable thickness.

Keywords: Micromanufacturing; Hole-flanging; Ironing; Size effect; Deformation behavior.

1. Introduction

During the last few decades, there appears a trend that products are fabricated more and more miniaturized with more micro/meso-scaled parts employed in different layers of product structured. This trend presents in many industrial clusters such as electronics, automotive, biomedicine and aerospace (Vollertsen et al., 2006). To meet these trends, various micro-manufacturing technologies have been intensively developed to meet the demands for miniaturized parts, which contains micro-machining, laser processing, lithography, micro-injection and microforming. Among these technologies, the microforming technology is a promising approach to producing microparts with the characteristics of near-net shape, desirable mechanical property, high productivity and low cost (Sato et al., 2015).

Despite the extensive study of microforming being conducted, the large-scale application of this unique micromanufacturing for mass production of microparts in industries is still not yet possible. This is due to some critical issues obstructing its wide application, such as the difficulty in handling of micropart or billet, stripping of final parts without damage, and positioning and transportation of preform in between the operation processes. To solve these problems and meet the increasing demands for the mass fabrication of microparts, the concept of progressive microforming was emerged and developed. Hirota (2007) firstly proposed a new method to fabricate small billets of 1 mm in diameter by extrusion process directly using sheet metal, and further investigated the relationship between the billet height and the constraining condition. On the basis of this novel method, further researches have been conducted. Chan and Fu (2013) fabricated the bulk cylinders and flanged parts using sheet metal in meso/micro scales, and examined the characteristics of the finished parts and production process. Based on the prior studies, Meng et al. (2015a) conducted further and extensive study of progressive microforming, and a custom-made micro-shearing process for progressive forming of microparts was analyzed. Ghassemali et al. (2013b) adopted this

process to produce axisymmetric parts with micro pin features. They also studied the variations of material flow and microstructure evolution induced by the size effect of microstructural grain diameter and specimen geometry.

As one operation in a progressive forming system, the hole flanging is used to produce a flange by facilitating the flow of the peripheral materials of a pre-pierced hole on the sheet into a die cavity. As a conventional forming process, hole-flanging is commonly applied to form hole feature with the strengthened edge, increase bearing surface and extend support for threads to fit other parts (Centeno et al., 2012). To obtain a higher flange, a method of hole flanging-ironing integrated process was developed, which is featured with a small gap between the punch and the die, as shown in Fig 1. In hole flanging-ironing process, the parts may fail with the occurrence of fracture, necking or tearing in the periphery of flange feature and many investigations on the limit of the hole expansion ratio (LER) were conducted. Huang and Chien (2001) put up a forming limit diagram showing that a linear relationship between the diameters of the maximum-expanded and initial hole. Hyun et al. (2002) investigated the hole flangeability of high-strength steel plate, and pointed out that both minimum hole diameter and lip shape accuracy are valuable for estimating the hole flangeability. Mori et al. (2010) enhanced the stretch flangeability of steel sheets by improving the forming quality of the punched edge. They stated that the LER is improved by optimizing the clearance between the die and the punch in piercing operation. Narayanasamy et al. (2010) correlated the mechanical properties and fractographic parameters with the LER of different automobile steels. They found that the void size and void area fraction affect the LER, and the material with big voids has a larger LER. Kacem et al. (2011) explored the effects of ironing and blank-holding force on the forming load, deformation kinematics and forming quality in the hole-flanging of aluminum alloy sheet. They argued that there is a critical clearance-thickness ratio of 0.68 to distinguish the hole flanging with or without

ironing. In addition, they determined the LER of hole flanging process by using the ductile fracture criteria (Kacem et al., 2015). Furthermore, Lin et al. (2007) presented a new method incorporating the features of counter-pressure in bulk extrusion and axially assisted forming to obtain a more substantial flange. Thipprakmas and Phanitwong (2012) discussed the deformation mechanism of hole-flanging and the effect of burr orientation on the forming quality of flanged parts. Soussi et al. (2016) analyzed the conventional hole-flanging process performed on the sheet metal of 0.8 mm by changing the clearance-thickness ratio and the initial hole diameter, and the effects of forming parameters on the geometrical dimensions of the flange including flange height, thickness distribution at the flange extremity and the flange state were also investigated. Cao et al. (2016) developed a new featured flanging tool to minimize the sheet thinning in incremental hole-flanging process. They stated that the new tool generates more meridional bending than stretching deformation, leading to more uniform thickness distribution of the finished workpiece. Brüning and Vollertsen (2012) firstly conducted the flanged forming process in micro range with the sheet thickness of 25 μm. They stated that the LER decreases with the sheet metal thickness, and the macro-scaled model is applicable to predict the flange height of micro-scaled flanged forming.

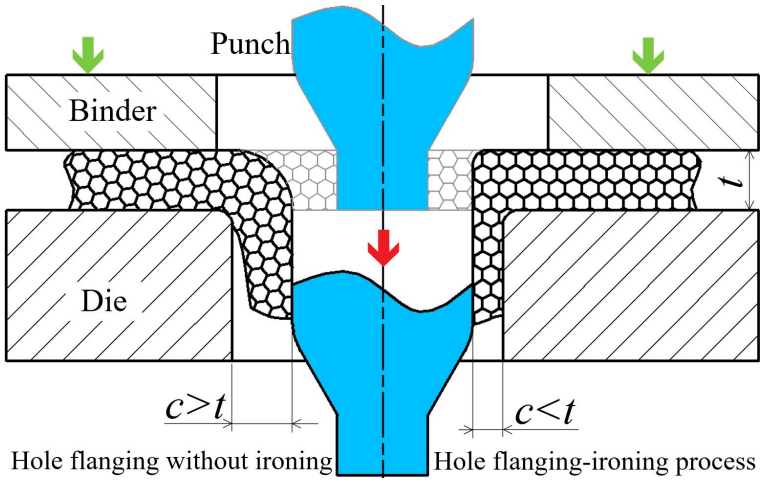

Fig. 1. Hole-flanging process with and without ironing.

According to the previous researches mentioned above, less attention has been paid to the investigation of size effect and deformation mechanism involved in the hole-flanging for the tiny initial hole and thin sheet metal. In addition, the application of hole-flanging in progressive microforming has not yet been explored and promoted. When the geometry of hole-flanging process is scaled down to meso/micro scenarios, the unpredictable results may appear. In this study, a comprehensive investigation of size effect on micro hole flanging-ironing during the progressive microforming process of an unequal-thickness micropart was conducted. The unique deformation behavior in the process chain including micro-scaled shearing, hole flanging with ironing and blanking was systemically explored. The forming quality, defect occurrence, dimensional accuracy, fractographic property and microstructure evolution related to size effect were finally examined. The research thus provides an in-depth understanding and a basis for the promising application of the process.

2. Material and the objective micropart

2.1. The testing material

Due to the excellent formability and extensive application in many industries, the pure copper sheet metal with the thickness of 0.4 mm was chosen as the experimental material. To investigate the grain size effect, the sheet was annealed in an inert gas-filled furnace to obtain different grain sizes, as listed in Table 1. The microstructures along the sheet plane and the cross-section in its thickness are shown in Fig. 2. All the microstructure images were captured by an optical microscope, after etching the surfaces by using the solution of $FeCl_3$ (5 g) + HCl (15 ml) + H_2O (85 ml) for 10 seconds. According to ASTM E112 standard, grain size measurements were conducted using the linear intercept method excluding the twin boundaries.

Table 1 Annealing conditions and different grain sizes of the testing material.

Annealing conditions	Dwelling time /h	Average grain size /μm	*t*/*d*
As-received	-	14.5±0.7	27.6
500 °C	2	36.9±2.3	10.8
600 °C	2	44.0±2.5	9.1
750 °C	3.5	67.7±3.9	5.9

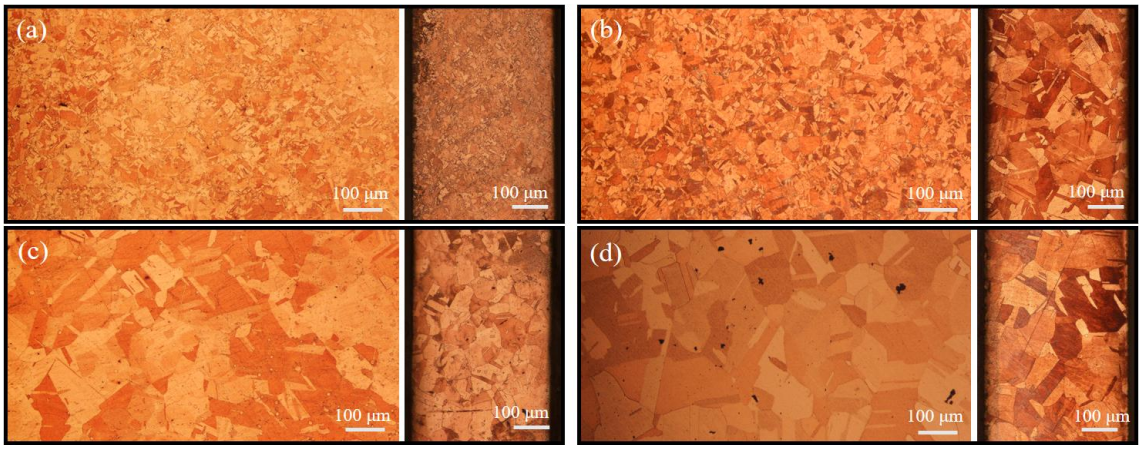

Fig. 2. Microstructures of the testing materials: (a) as-received; (b) 500 °C annealed; (c) 600 °C annealed and (d) 750 °C annealed.

To acquire the mechanical properties of the metal sheets with diverse microstructures, the tensile tests were conducted on a testing machine. To improve the accuracy of the experimental results, three tests were performed for each material condition. According to ASTM standard, the dimensions of the test specimen are designed, as shown in Fig. 3. A standard extensometer with the length of 25 mm was applied to measure the extension precisely. The velocity of the crosshead was set as 0.033 mm/s for all the tests. The strain-stress curves of pure coppers with diverse initial microstructures are also shown in Fig. 3.

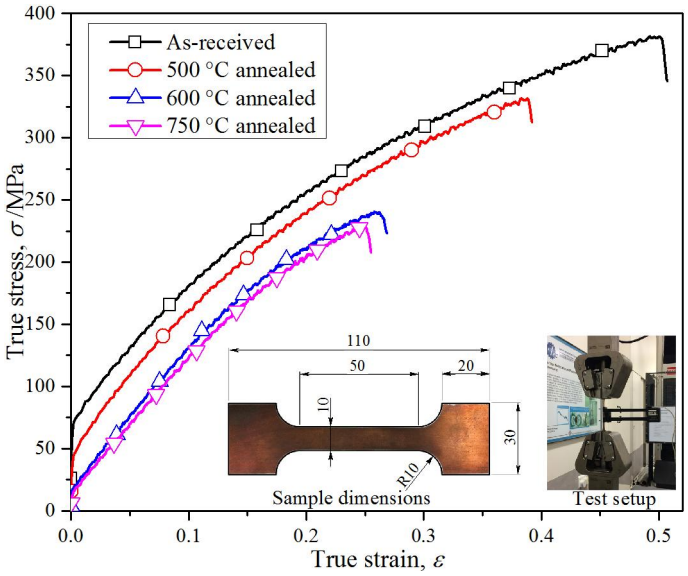

Fig. 3. The strain-stress curves of pure coppers with diverse initial microstructures.

2.2. Geometrical features of the micropart

To explore the deformation mechanism, dimensional accuracy, fractographic property and microstructure evolution in the micro-scaled hole-flanging process with ironing, a micro-scaled flanged part was designed as the case study and its dimensions are shown in Fig. 4. It is found that the thickness distribution between the non-deformed part and the straight wall is uneven. The unequal-thickness microparts fabricated by forming technologies are widely applied in the occasions of fastening, junction and electrode due to the continuous distribution of metallic flow line and desirable mechanical performance. However, the obstacle in high production and quality has not been overcome due to the irregular material flow and the difficulties in handling, transportation, positioning and ejection of the workpiece at micro scale.

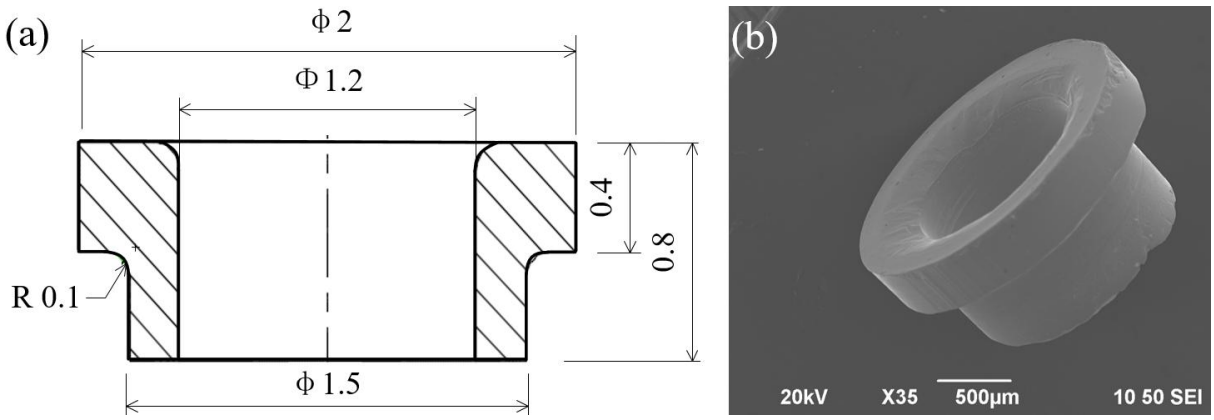

Fig. 4. The unequal-thickness micropart and its dimensions: (a) geometrical dimensions and (b) photo of the deformed part by scanning electron microscope (SEM).

3. Experimental Methods

3.1. Determination of hole flanging-ironing parameters

To realize the integrated hole flanging-ironing process in the progressive microforming system, the tool geometry parameters are needed to be carefully designed. The geometrical parameters of die tooling are presented in Fig. 5, and the designed values are shown in Table 2. In Fig. 5, the clearance between the punch and the die determines whether the hole-flanging is conducted with or without squeezing, which is defined as follows:

$$c = \frac{1}{2}\left(D_f - d_f\right) \tag{1}$$

In addition, the notation, R_c, defined as the ratio of die clearance c to sheet thickness t in Eq. (2), decides the occurrence of ironing deformation.

$$R_c = \frac{c}{t} \tag{2}$$

there is a critical value of R_c to distinguish the two flanging conditions. In the hole flanging process with ironing, the clearance is set less than a critical value. For a given workpiece thickness t, the critical value of R_c can be determined using the following equation (Kacem et al., 2011):

$$0.5tR_c^3 + \frac{d_f}{2}R_c^2 - \frac{d_p}{2} = 0 \quad (3)$$

the critical value derived from Eq. (3) equals to 0.7, which means that the ironing deformation occurs in the developed hole-flanging process because the ratio of punch-die clearance to the sheet thickness is 0.375, which is lower than the calculated critical value.

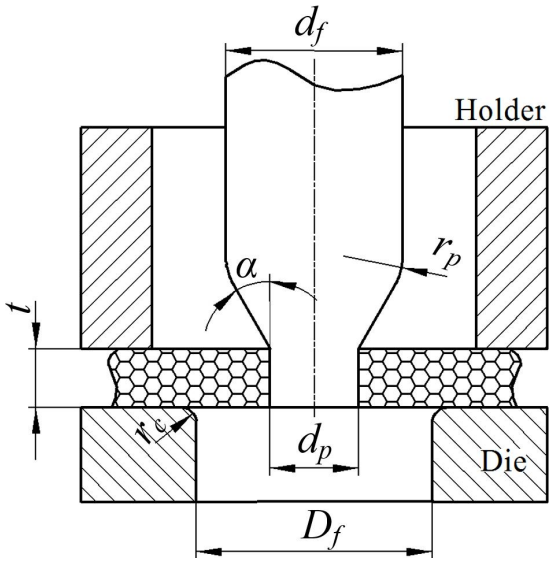

Fig. 5. Tool geometrical parameters of the hole flanging-ironing process.

Table 2 Tool geometry parameters used in the hole flanging-ironing integrated process.

Nomenclature	Symbol	Designed values
Diameter of the initial hole	d_p	0.6
Strip thickness	t	0.4
Punch diameter	d_f	1.2
Cone semi-angle of the punch	α	30°
Punch profile radius	r_p	0.4
Die diameter	D_f	1.5
Die profile radius	r_c	0.1
Clearance	c	0.15

3.2. Experimental produces

The developed progressive micro forming system consists of three forming steps, viz. shearing, hole-flanging with ironing and blanking, as shown in Fig. 6. All the steps are

realized by using different sets of tools. A copper sheet trimmed as a long strip is placed in the first position. In the first operation, a micro-hole is punched and a micro-pin is blanked out. Due to the fact that the punching process significantly affects the frangibility and the fine blanked hole is preferred for achieving better-flanged shape (Thipprakmas et al., 2007), the unilateral clearance between the punch and the die is set to be 10 μm, which is 2.5% of the sheet thickness and far samller than that of the conventional punching process. During the second operation, the pre-pierced hole is used for positioning and a long flange is formed by micro-scaled hole flanging-ironing process. The workpiece after the first two operations is connected with the original metal sheet, and the positioning and transportation of the preforms are replaced by the handling of the material sheet. When the second stage is finished, the sheet metal is fed to the third station. In the third stage, a flanged part is trimmed out. In addition, there is no overlap among the three working operations in one stroke by adjusting the punch length in each step, and the metal sheet moves forward continuously at an interval of each stroke. Consequently, the progressive microforming process is realized, and the finished microparts are produced continuously. The experiments were conducted by operating a programmable MTS machine mounted a load cell with the capacity of 25 kN. All tests were conducted at a velocity of 0.01 mm/s to ensure a quasi-static state and avoid the effect of strain rate. The material for tooling fabricating is chosen as high-speed steel, SKH-51. To further characterize the grain size effect on the dimensional accuracy of the flanged part, three workpieces were manufactured and measured under the same condition.

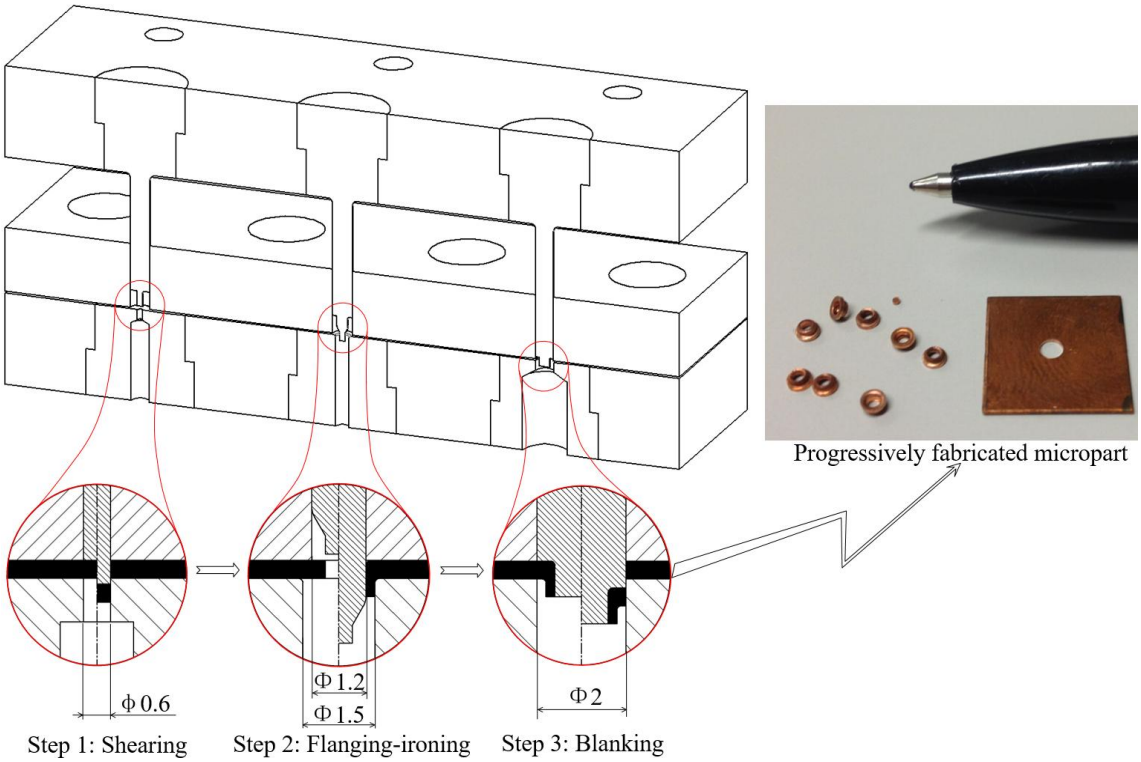

Fig. 6. The experimental die layout and the finished microparts.

4. Results and discussion

4.1. Deformation load and forming kinematics

In micro/meso-scaled forming process, the material microstructure is one of the key parameters affecting the deformation load, forming kinematics, dimensional accuracy and final morphology of the finished part. Fig. 7 presents the relation between the material condition and the punch load. There are three forming operations in the developed progressive microforming chain designed. In the first step, the work material is subjected to shearing deformation, and a micro-pin and a pierced hole are produced after the punch stroke reaches 0.4 mm. The second operation is the hole flanging-ironing integrated process with the punch travel ranging from 0.4 to 2.0 mm used to fabricate the flanged micropart. In the third step, the punch stroke spanning from 2.0 to 2.4 mm stands for the blanking process. It is found that the punch load in the whole progressive forming process decreases with the

increasing grain size, while there is no obvious relationship between the punch travel at the peak load and grain size.

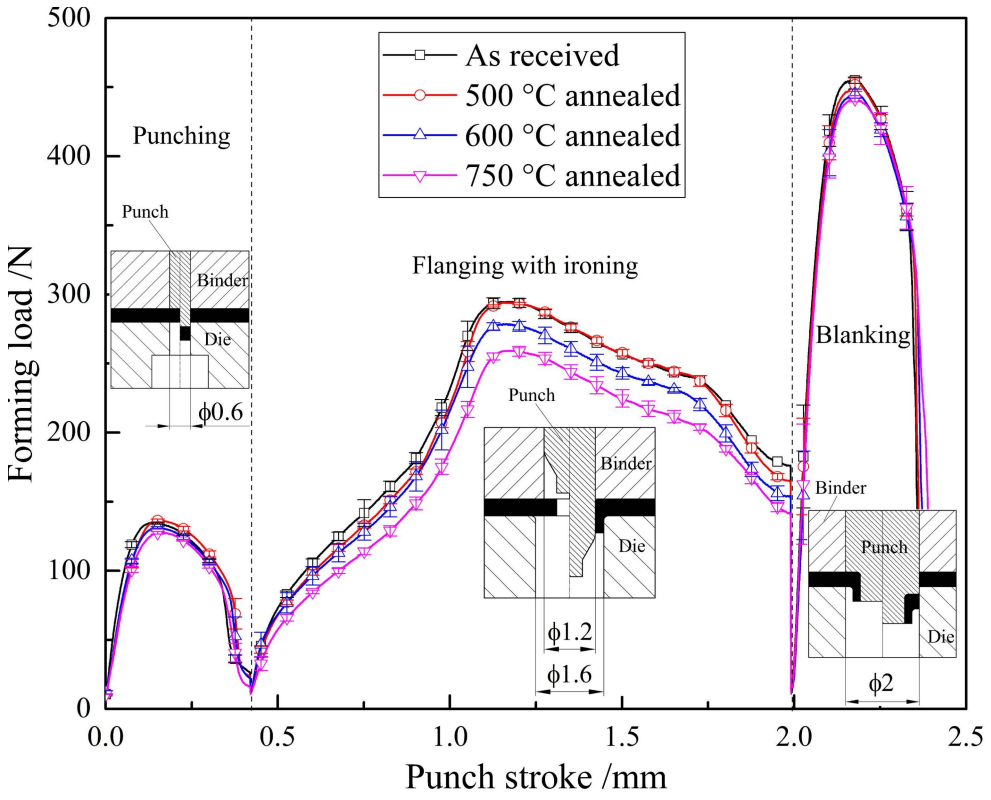

Fig. 7. Load-stroke curves of micro hole flanging-ironing under different grain sizes.

To further analyze the forming kinematics in the micro-scaled hole flanging-ironing process, the variation of the deformation load and the corresponding deformed shapes are presented in Fig. 8. It is shown that five deformation stages including elastic deformation, deflexion, flow forming, ironing and sliding are identified in the micro-scaled hole flanging-ironing process, which is similar to the macroscopic flanging process with ironing as shown in the work of Kacem et al. (2011). In the first stage, the metal sheet is subject to elastic deformation, and the punch load grows linearly. The second stage begins with the accentuation of plastic deformation and ends up with the contact between the round surface of the punch and the top surface of the workpiece. The deflexion of the hole edge becomes the dominant deformation pattern characterized by a nonlinear growth of the punch load. The third stage starts from the accumulative deflection deformation of hole edge, and the testing

material is pushed down to flow towards the die orifice. The punch load achieves the maximum due to the severe plastic deformation in this stage. During the ironing stage, the testing material is squeezed to fill the clearance between the die and the punch. In the last stage, the sliding between the punch and the inner surface of the flange takes place, and the deformation pressure drops significantly. On the other hand, it is noted that deformation load increases with the reducing grain size, which is caused by plenty of dislocations to accomplish the flanging and ironing deformations. With the increasing grain size, the scatter of punch load increased, which is attributed to the enhanced anisotropies of material deformation with coarse grains.

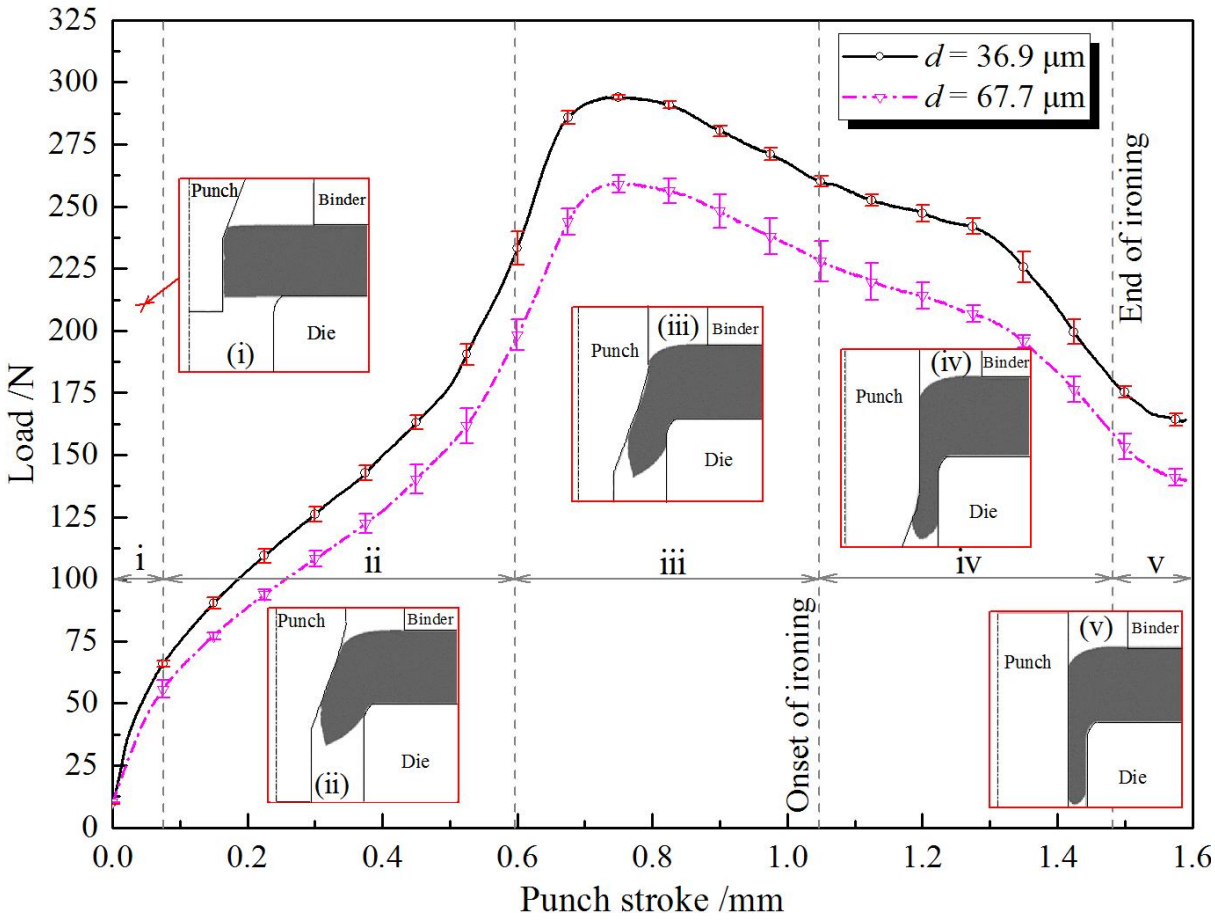

Fig. 8. Forming kinematics of the hole flanging-ironing process.

4.2. Geometric size effect

4.2.1. Cylindrical micro-pin

By using the developed progressive microforming process, two microparts were fabricated in single stroke including a micro-pin in the shearing pass and a flanged part in the hole-flanging step. The micro-pin produced by the shearing operation from the sheet metal can be used as the micro billet for the characterization of material deformation behavior, as shown in the work of Ghassemali et al. (2015). To explore the size affected surface morphology and the final shape of micro-pin obtained from the micro-shearing process, two shearing processes with diverse dimensions were designed and demonstrated in Fig. 9. For scenario I, the diameters of the punch and die are 0.74 and 0.785 mm, respectively, while the punch-die clearance in one side is 22.5 μm. For scenario II, the diameters of the punch and die are 0.6 and 0.62 mm, respectively with the punch-die clearance of 10 μm.

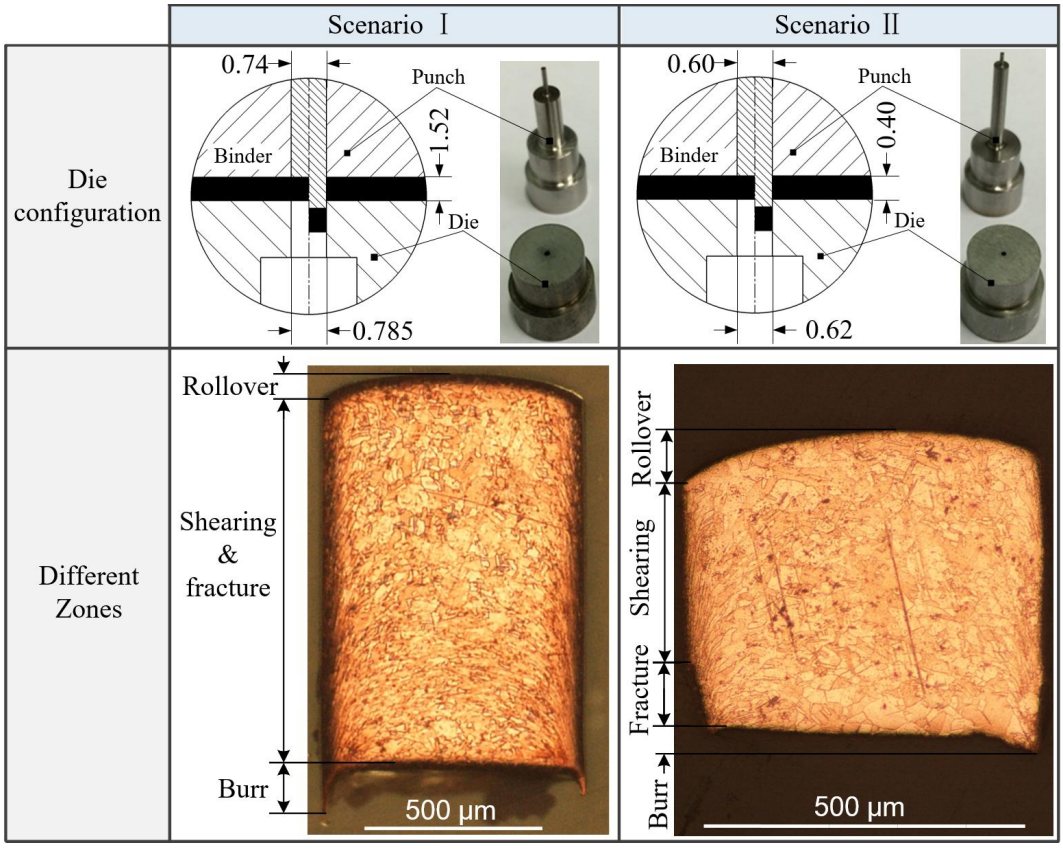

Fig. 9. Different zones of the fabricated billets.

The cylindrical micro-pins can be characterized by the distinct zones including rollover, burnish zone, fracture zone and burr respectively, as defined in Meng et al. (2015b). To determine the size effect on the profile of the sheared micro-pins, the zone distributions of the fabricated micro-pins using different materials with various grain sizes are presented in Fig. 10. It is observed that the forming quality of sheared micro-pin is influenced by both blank thickness and material microstructure, and burnish zone diminishes with the increasing grain size and miniaturized thickness. On the other hand, the miniaturization affects the proportion of the distinct zones considerably. However, the distribution of the fracture and burr zones seems to change slightly with grain size for the two scenarios. For the 750 °C annealed material with the thickness of 0.4 mm, however, the section shape of sheared pin differs from conventionally-known one. The shear zone is not dominant and relatively large rollover and fracture zones are formed, which is due to the large size of grains along the thickness direction of work metals (Joo et al., 2005).

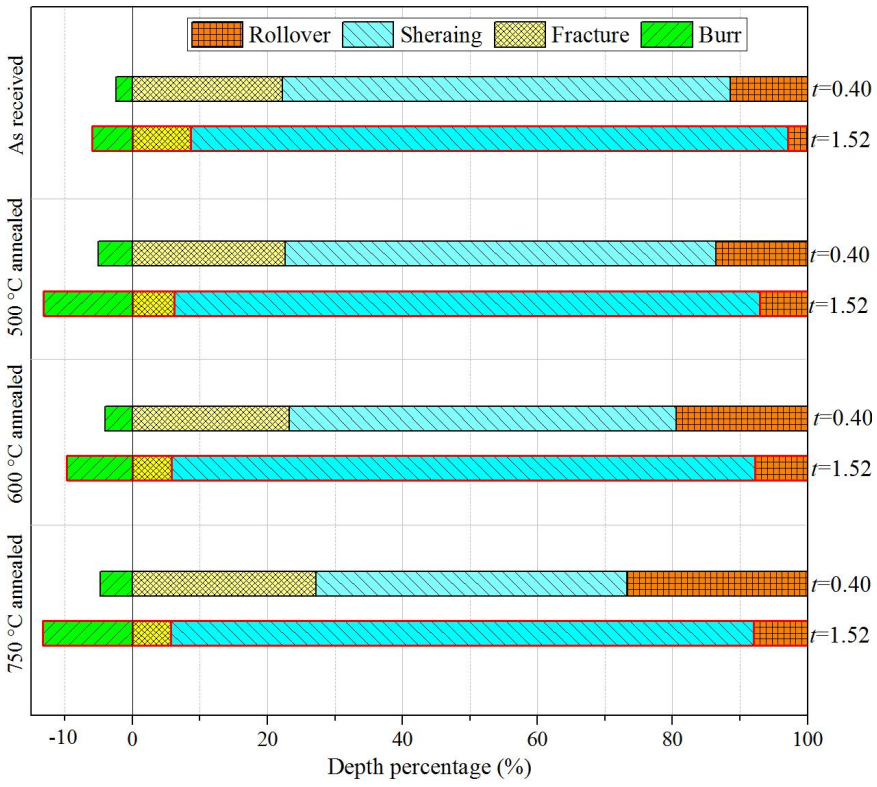

Fig. 10. Distributions of different zones of the sheared pin under diverse material conditions.

Fig. 11 shows the comparison of the fabricated micro-pins under different material conditions. It appears that the length of cylindrical pin decreases with the increasing grain size, which is attributed to the aggravated lateral material flow when using the coarse-grained material. In addition, the pin shape becomes much more irregular with the increase of grain size, which reduces the dimensional accuracy of the fabricated part. The occurrence of irregularities of coarse-grained material is related to the limited formability of few grains in the deformed zone. Kals and Eckstein (2000) revealed that the irregular pin surface is generated when there are only one or few grains across the thickness direction and the grain orientation is unfavorable to deformation along the shearing direction. When the grain size is comparable to the sheared micro-pin, the property of individual grain becomes dominant, and the anisotropy of individual grain promotes the heterogeneous deformation and anisotropic slip. Therefore, there is a strong size effect on the material deformation behavior in the shearing process, and the fine-grained material is preferred to obtain a persistent smooth burnish zone.

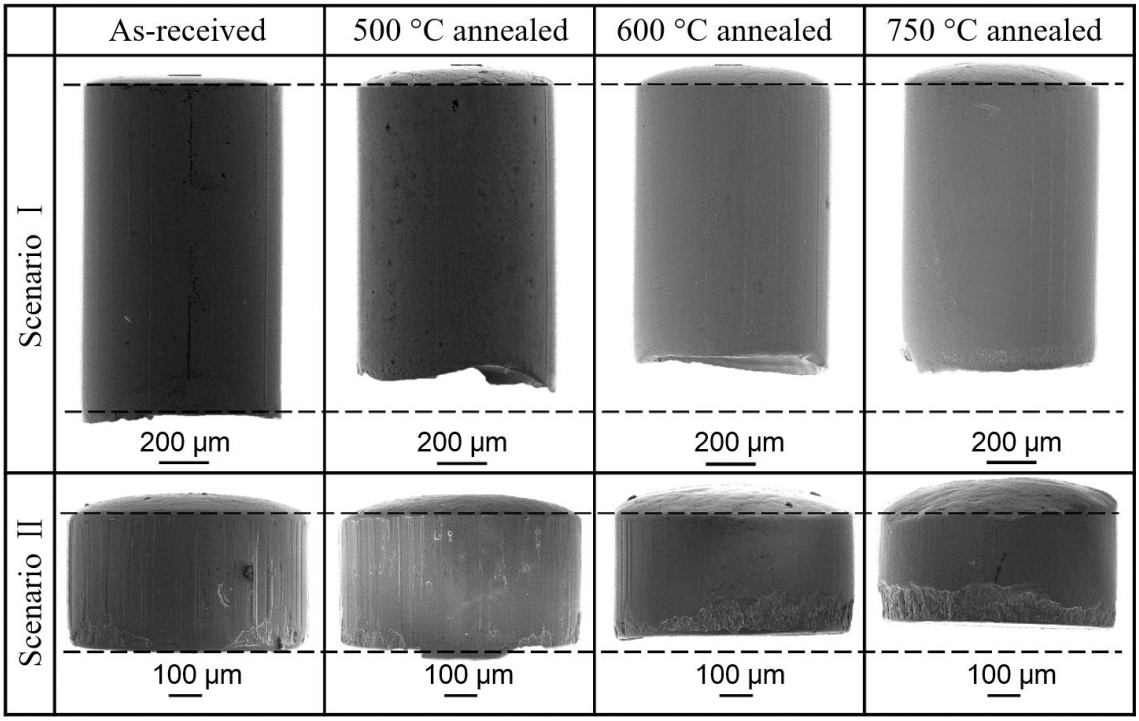

Fig. 11. Comparison of the length and final shape of the fabricated micro-pins.

4.2.2. Hollow flanged micropart

Like other forming technologies, the integrated hole flanging-ironing process is restricted by the occurrence of diverse defects. To study the forming quality of the flanged micropart, the surface morphology of the flanged edge was observed via SEM, and the typical flaws are shown in Fig. 12. It is found that the flanged microparts fabricated using fine-grained materials has the desirable forming quality. The surface integrity of the formed part worsens with the increasing grain size, and the incontinuity and irregularity occur when the grain size is greater than 36 μm. Meanwhile, the surface integrity of the junction between the flanged edge and the non-deformed zone also changes with grain size. For the as-received materials, the junction surface presents a desirable asperity, while the surface for the coarse-grained material becomes rough. This phenomenon can be explained by the size effect on crystal plasticity. When the size of the working material is in microscale, there are few grains constituting the deformation body and the stochastic distribution of various grains is weakened. Consequently, the anisotropy of single grain becomes dominant, and the grain prefers to deform along the favorable direction, leading to the inhomogeneous deformation (Meng and Fu, 2015).

In addition, the dimple and wrinkling were observed on the surface of the flanged tip. The wrinkling phenomenon is a flow-induced defect caused by the inhomogeneous material flow behavior defined in Wang et al. (2013), while the dimple is resulted from the void growth and nucleation. In the micro hole-flanging process, the ductile fracture is easier to occur due to the accumulated deformation caused by shearing for obtainment of the initial hole. Kacem et al. (2013) found that microvoids and necking exist before ironing in the flanging process, and the ironing process tends to close the existing voids due to the sudden drop of stress triaxiality from about 0.33 to -0.6 caused by the compressive state. Consequently, the microvoids appear before ironing stage, and the dimples are formed due to

the void closure after squeezing deformation. Furthermore, the dimples, wrinkling and irregularities worsen at the flanged tip with the reducing number of grains across the thickness of the working material. Since the workpiece is squeezed between the punch and the die in ironing process and when the coarse-grained material is used, the inconsistent deformation among the anisotropic grains is more liable to occur, leading to the aggravated irregularities but not tearing.

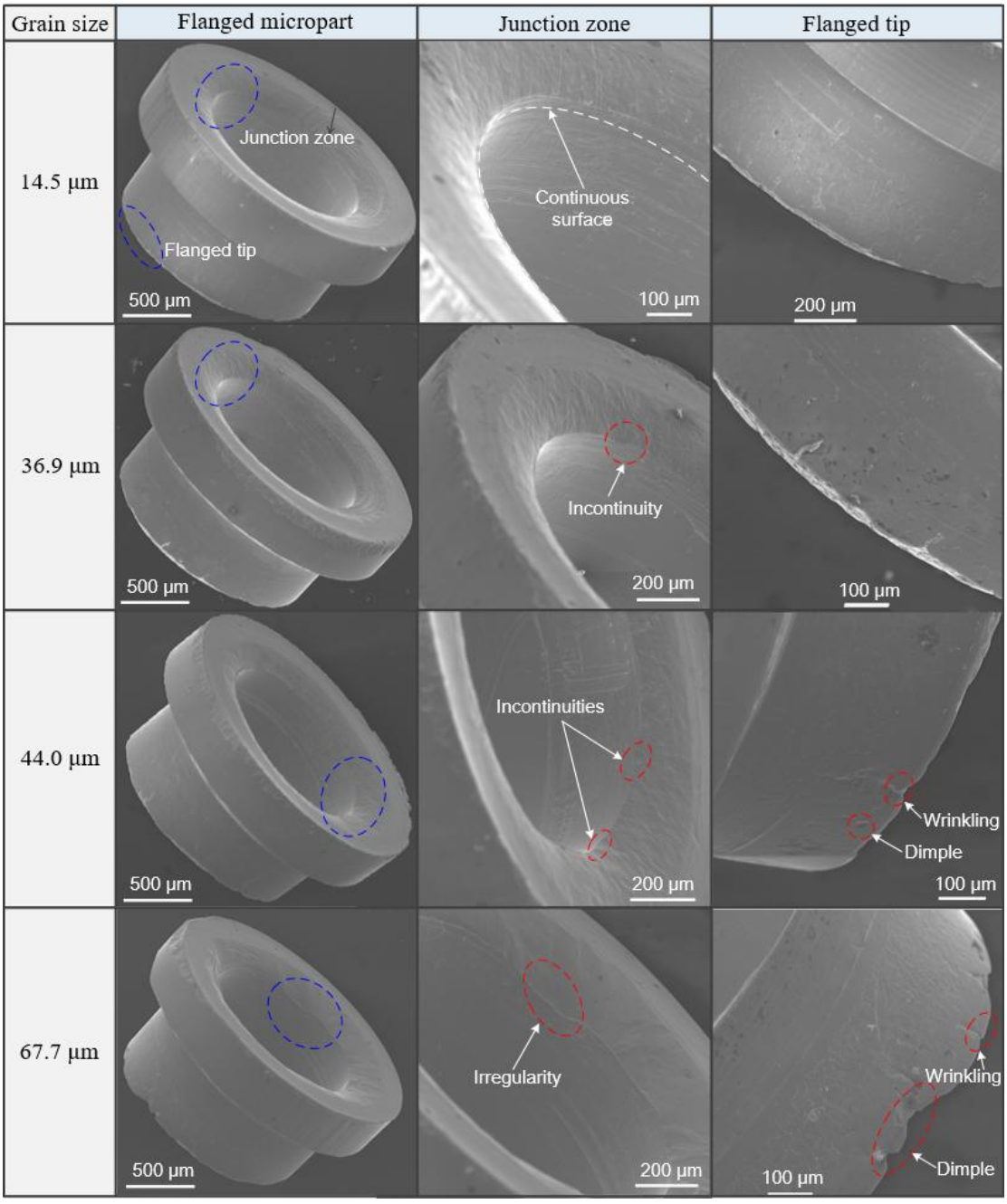

Fig. 12. Change of surface integrity with grain size.

To quantificationally analyze the dependence of the forming quality of the flanged micropart on material microstructure, the dimensional accuracy of the micro flanged part was examined. Fig. 13(a) shows the change of the flange height H_1 with grain size. It is appeared that the average height of flange decreases from 0.65 to 0.60 mm with the increasing grain diameter, which could be attributable to the slight ease of material flow into the die cavity when using the material softened by annealing treatment. In other reports, however, the marginal effect of grain size on the length of microparts was found when a micro-pin was produced with the diameter of 0.3 mm from the strip with the thickness of 2.5 mm (Ghassemali et al., 2015). This is because there are sufficient materials in the thickness direction to flow into the die orifice due to the thick strip. Nevertheless, the lateral material flow takes up a considerable proportion with few grains across the thickness direction, leading to a distinct variation of the length of the fabricated flange with initial grain size. On the other hand, the standard deviation is generally increased with grain size due to the enhanced irregularities at flange tip induced by the variation of grain orientations in the coupled deformation mode of edge stretching, bending and extruding.

It is deduced from the cross profile of the finished micropart that there is a height difference existing between the inner and outer surfaces of the flange. To evaluate the changing tendency of the height difference, the inclination angle between the inner end and outer tips was measured, as presented in Fig. 13(b). The results reveal that both tapering angle and the scatter increase with grain size. The inclination angle for the micropart with the as-received material is about 27°, while it is increased to 38° for the material annealed at 750 °C with the average grain size of 67.7 μm, and the increment rate is up to 33.3％.

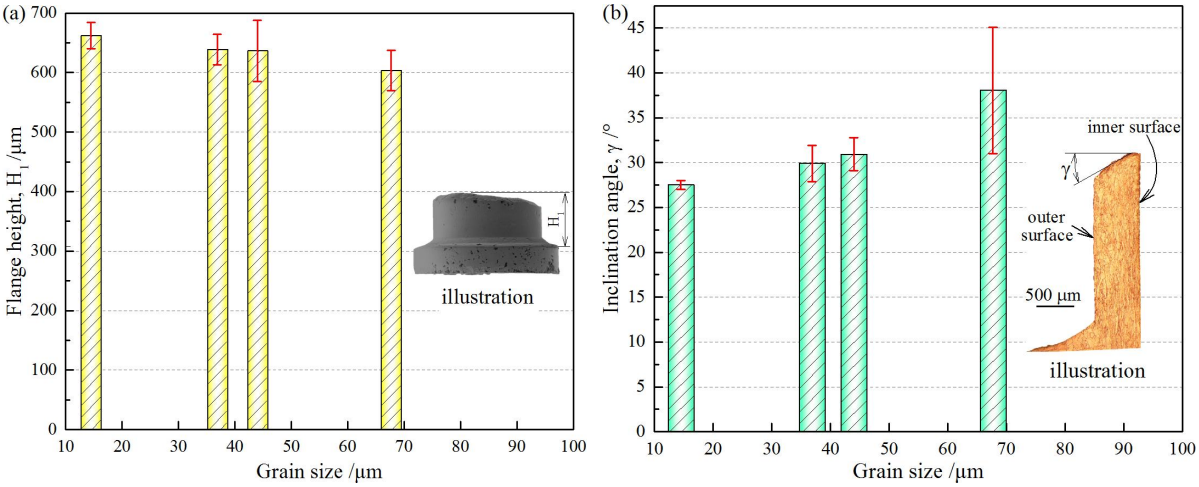

Fig. 13. Effect of grain size on the geometric dimensions of the flanged part: (a) flange height, and (b) tapering angle between inner and outer surfaces.

The inclination phenomenon at the flange tip can be explained by the coupling effects of free surface roughening and open and closed lubricant pockets, as illustrated in Fig. 14. When the working material is deformed before squeezing in the hole flanging-ironing process, the free surface between the punch and the blank-holder does not contact with the tools. The grains are less constrained in the free surface, and the surface of the workpiece becomes rough with the increasing plastic strain, which is called free surface roughening phenomenon (Furushima et al., 2014). Meng and Fu (2015) emphasized that the surface nonuniformity induced by the free surface roughening is aggravated with the increase of grain size. Abe (2014) stated that the wavelength of the generated surface roughening curve is approximately ten times of the average grain diameter. Compared with the fine-grained material, the free surface roughness with coarse-grained material is relatively severe with a large interval between the roughness valley and peak before the onset of ironing, as presented in Fig. 14. As the punch moves forward, the squeezing deformation is dominant, and the deformation load is applied to the contact surface. The lubricant on the asperities at the two edges of the contact surface was squeezed out from the valley, leading to the formation of open lubricant pocket (OLP). On the contrary, the lubricant is stuck in the roughness valley and the closed

lubricant pocket (CLP) is generated at the middle zone of the contact surface. The regions around the OLPs and CLPs were flattened by the forming load, increasing the real contact area (RCA) and friction (Chan et al., 2011). In the CLP, the pressurized lubricant prohibits the deformation of asperities. With the increasing grain size, the fraction of the generated roughness valley resulted from the free surface roughening is reduced. Consequently, the share of OLPs is expanded, and the ratio of RCAs to CLPs is thus increased, leading to a high interfacial friction between the punch and the cylindrical boring. Whereas, for the fine-grained material with a large portion of CLPs, the generated hydrostatic pressure prohibits the deformation of the inner surface, which reduces the degree of surface flattening. The friction between the inner surface and the punch is lower, and the material flow along the punch surface is slowed down. Therefore, the height of the inner surface of the workpiece with coarse grains is larger than that with fine grains at the same punch stroke, resulting in a high inclination between the inner and outer tips.

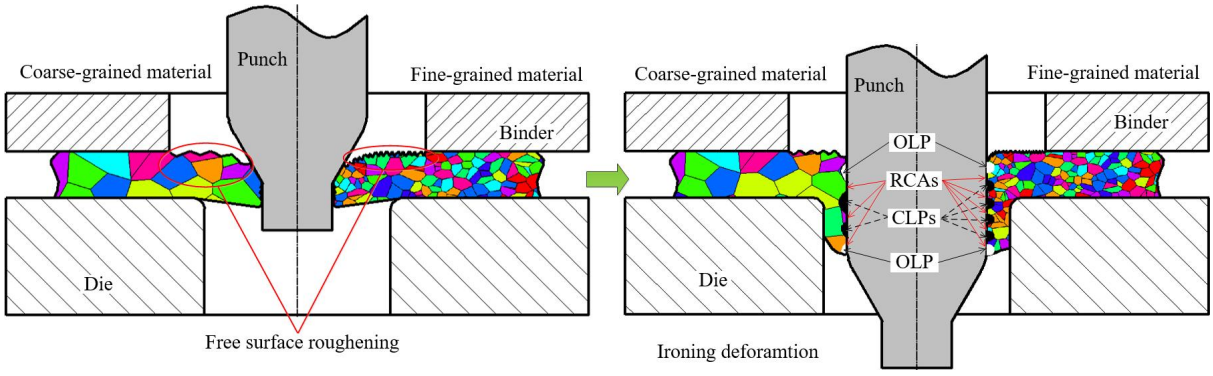

Fig. 14. Schematic illustration of the free surface roughening and the lubricated effect on the tapering angle.

Compared to macro-scale hole flanging, there are some new elements that aggrandize the complexity of the process including accumulative deformation and heterogeneous material flow in the miniaturized and integrated progressive flanging-ironing process. Three workpieces were manufactured and measured under the same condition to describe the grain size effect on the diametrical accuracy. The change of the diameter of the flanged microparts

is illustrated in Fig. 15. In this figure, the diameter of blanked edge, outer and inner diameters of the flange are denoted by D_1, D_2 and D_3, respectively, and the designed values of D_1, D_2 and D_3 are 2.0, 1.5 and 1.2 mm, as presented in Fig. 4. It is found that the material microstructure has a less impact on the diametrical distribution of the flanged micropart, compared with the variation of the flange length with grain size. This is because the deformation along the diametrical direction is restricted by die tooling in the process, whereas the working materials deform freely along the longitudinal direction. In addition, all the relative standard deviations of the three diameters are samller than 3%, which further indicates the marginal influence of grain size on the diametric dimensions. However, the scatter of the diameters is increased by using the annealed materials due to the different flow patterns of work material between the fine- and coarse-grained materials.

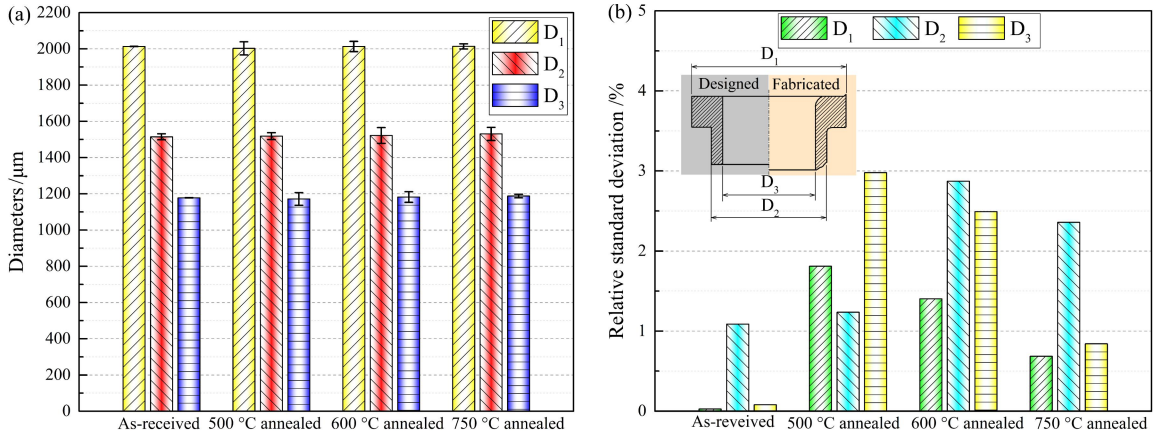

Fig. 15. Effect of grain size on the diametrical distribution of the finished micropart: (a) diameters and (b) relative standard deviation.

4.3. Microstructure evolution

The observation of microstructure evolution in the progressive hole flanging-ironing process was done using an optical microscope. Fig. 16 shows the microstructure evolution in the first step of the progressive microforming, i.e., micro-scale shearing process. It is found that the initial grain size influences the microstructure of the blanked micro-pin significantly. In addition, the morphology of the micro-pin becomes irregular with increasing grain size due

to the fact that the random orientation and anisotropic property of individual grains strengthen the inhomogeneous deformation and asymmetric geometry. In addition, the shear band becomes obscure with the reducing number of grains involved in the shearing deformation, leading to a wavy side edge of the micro-pin with coarse-grained material. Whereas, the grains anisotropies of the fine-grained materials are averaged and there are sufficient grains participating in the deformation zone, resulting in more materials to flow in the shearing direction and accomplish the deformation.

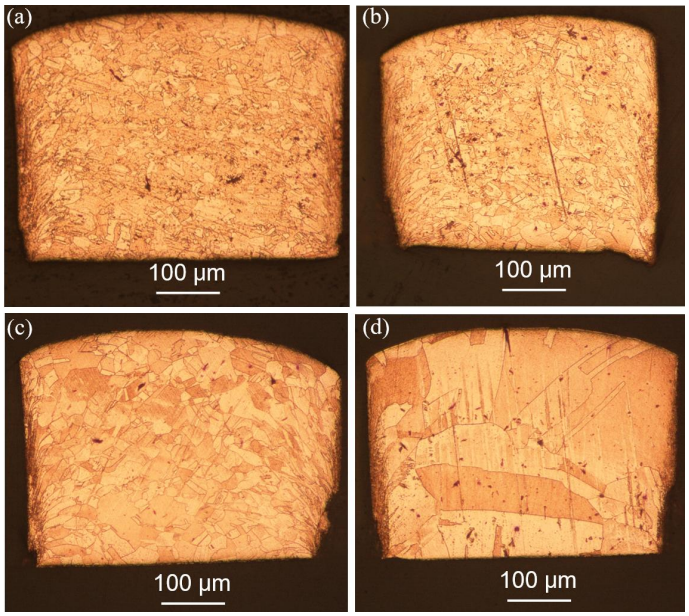

Fig. 16. Microstructure evolution in micro-scale shearing process with different initial grain sizes: (a) 14.5; (b) 36.9; (c) 44.0 and (d) 67.7 μm.

To characterize the evolution of microstructure in the integrated hole flanging-ironing process, observations of the sectional microstructure of the flanged micropart were conducted for each material condition. The sectional microstructures are shown in Fig. 17. It is seen that the hole flanging-ironing process produces a flanged feature with a curved profile followed by a straight wall, and short curved profile and desirable boring straightness are achieved by using the fine-grained material. In Fig. 17, zone I is the junction between the blanked part and the flanged edge, and the demarcation lines were observed to distinguish the bending region and the zone of edge stretching and ironing deformation for the as-received and 500 °C

annealed materials. The inhomogeneous microstructure distributions are induced by the formation of dead zone, which is affected by the geometry and friction effects (Ghassemali et al., 2013a). However, the separatrix becomes blurred for 600 and 750 °C annealed materials. This phenomenon is caused by the decrease of grain number involved in the deformation zone when the grain size is equivalent to the geometrical dimension of the workpiece. Zone II represents the obtained hollow cylinder, and no apparent defect is found at the cylindrical boring for all the material conditions, which is consistent with the findings of Kacem et al. (2015). Conversely, singularities were observed at the outer profile of the flanged edge using the coarse-grained material. This could be attributed to the loss of grain number and enhanced anisotropic properties of individual grains. In addition, the threadlike microstructural morphology is found on the workpiece using fine-grained material due to the fact that the work material is squeezed with a full contact between the punch and the die. With the increase of grain size, the slip direction of individual grain could be different from the ironing direction, leading to the inconspicuous ironing deformation. It is found from zone III that the generated irregularities at the flanged tip is intensified with the increasing grain size, which agrees well with the change tendency of inclination angle versus grain size, as shown in Fig. 13(b).

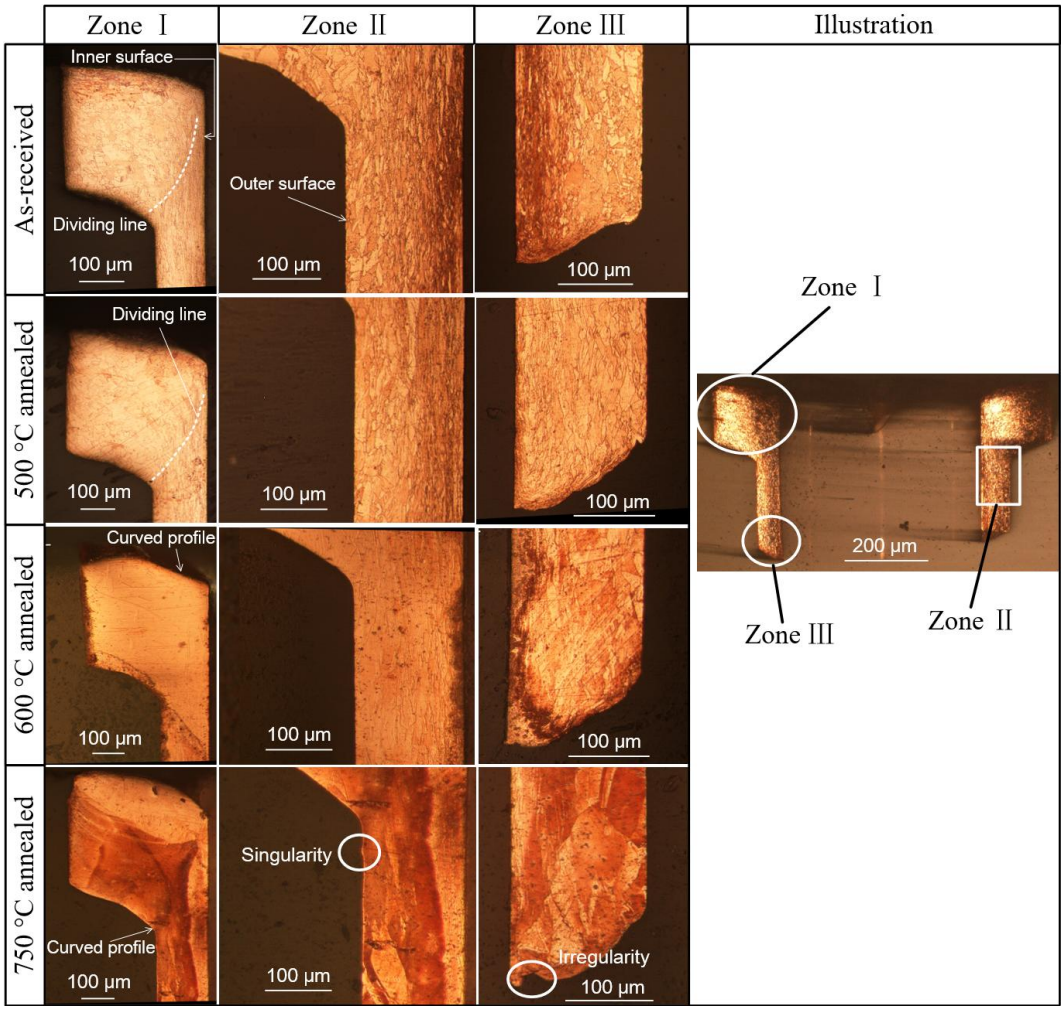

Fig. 17. Microstructural evolution in the integrated micro-scale hole flanging-ironing process.

5. Conclusions

In this research, the micro-scale progressive forming system is developed for the substantial manufacturing of a variational-wall-thickness micropart by using an integrated hole flanging-ironing process, and its characteristic was explored from the aspects of deformation load, forming kinematics, dimensional accuracy, defect formation and microstructural evolution. Through careful examination of the developed progressive microforming system and the finished micropart, the following conclusions are therefore drawn from the present investigations.

(1) Five deformation stages including elastic deformation, deflexion, flow forming, ironing and sliding are identified in the integrated micro-scaled hole flanging-ironing process.

The deformation load of the whole progressive microforming decreases with the increasing grain size, while the scatter of deformation load is exacerbated.

(2) The surface quality of fabricated micro-pin is affected by both the workpiece thickness and material microstructure. The burnish zone and the length of micro-pin diminish with the increasing grain size and miniaturized thickness. With the increase of grain size, the shear zone is not dominant and the severe irregularities appeared, which is related to the limited formability of few grains involved in the shear deformation.

(3) The length of the formed flange is reduced with the increasing grain size, while both tapering angle and its scatter present an opposite tendency, which could account for the coupling effects of free surface roughening and open and closed lubricant pockets.

(4) The demarcation line is observed to distinguish the bending region and the zone of edge stretching and extruding deformation, which becomes blurred with the increasing grain size. In addition, the defects including curved profile, singularity and irregularity appear in the workpiece using the coarse-grained material, which is attributed to the decrease of grain number and the strengthened anisotropic properties of individual grains.

Acknowledgements

The authors would like to acknowledge the funding support to this research from the National Natural Science Foundation of China (Grant Nos.: 51575465, 51605018 and 51635005) and the project of 152792/16E (B-Q55M) from the General Research Fund of Hong Kong Government.

References

Abe, T., 2014. Surface roughening and formability in sheet metal forming of polycrystalline metal based on r-value of grains. International Journal of Mechanical Sciences 86, 2-6.

Brüning, H., Vollertsen, F., 2012. Mechanical flange forming in steel and copper foil. Production Engineering 6, 551-558.

Cao, T., Lu, B., Ou, H., Long, H., Chen, J., 2016. Investigation on a new hole-flanging approach by incremental sheet forming through a featured tool. International Journal of Machine Tools and Manufacture 110, 1-17.

Centeno, G., Silva, M.B., Cristino, V.A.M., Vallellano, C., Martins, P.A.F., 2012. Hole-flanging by incremental sheet forming. International Journal of Machine Tools and Manufacture 59, 46-54.
Chan, W.L., Fu, M.W., 2013. Meso-scaled progressive forming of bulk cylindrical and flanged parts using sheet metal. Material & Design 43, 249-257.
Chan, W.L., Fu, M.W., Yang, B., 2011. Study of size effect in micro-extrusion process of pure copper. Materials & Design 32, 3772-3782.
Furushima, T., Tsunezaki, H., Manabe, K.I., Alexsandrov, S., 2014. Ductile fracture and free surface roughening behaviors of pure copper foils for micro/meso-scale forming. International Journal of Machine Tools and Manufacture 76, 34-48.
Ghassemali, E., Jarfors, A.E.W., Tan, M.J., Lim, S.C.V., 2013a. On the microstructure of micro-pins manufactured by a novel progressive microforming process. International Journal of Material Forming 6, 65-74.
Ghassemali, E., Tan, M.J., Jarfors, A.W., Lim, S.C.V., 2013b. Progressive microforming process: towards the mass production of micro-parts using sheet metal. International Journal of Advanced Manufacturing Technology 66, 611-621.
Ghassemali, E., Tan, M.J., Wah, C.B., Lim, S.C.V., Jarfors, A.E.W., 2015. Effect of cold-work on the Hall–Petch breakdown in copper based micro-components. Mechanics of Materials 80, Part A, 124-135.
Hirota, K., 2007. Fabrication of micro-billet by sheet extrusion. Journal of Materials Processing Technology 191, 283-287.
Huang, Y.M., Chien, K.H., 2001. The formability limitation of the hole-flanging process. Journal of Materials Processing Technology 117, 43-51.
Hyun, D.I., Oak, S.M., Kang, S.S., Moon, Y.H., 2002. Estimation of hole flangeability for high strength steel plates. Journal of Materials Processing Technology 130–131, 9-13.
Joo, B.Y., Rhim, S.H., Oh, S.I., 2005. Micro-hole fabrication by mechanical punching process. Journal of Materials Processing Technology 170, 593–601.
Kacem, A., Krichen, A., Manach, P.Y., 2011. Occurrence and effect of ironing in the hole-flanging process. Journal of Materials Processing Technology 211, 1606-1613.
Kacem, A., Krichen, A., Manach, P.Y., 2015. Prediction of damage in the hole-flanging process using a physically based approach. International Journal of Damage Mechanics 24, 840-858.
Kacem, A., Krichen, A., Manach, P.Y., Thuillier, S., Yoon, J.W., 2013. Failure prediction in the hole-flanging process of aluminium alloys. Engineering Fracture Mechanics 99, 251-265.
Kals, T.A., Eckstein, R., 2000. Miniaturization in sheet metal working. Journal of Materials Processing Technology 103, 95-101.
Lin, H.S., Lee, C.Y., Wu, C.H., 2007. Hole flanging with cold extrusion on sheet metals by FE simulation. International Journal of Machine Tools and Manufacture 47, 168-174.
Meng, B., Fu, M.W., 2015. Size effect on deformation behavior and ductile fracture in microforming of pure copper sheets considering free surface roughening. Materials & Design 83, 400-412.
Meng, B., Fu, M.W., Fu, C.M., Chen, K.S., 2015a. Ductile fracture and deformation behavior in progressive microforming. Materials & Design 83, 14-25.
Meng, B., Fu, M.W., Fu, C.M., Wang, J.L., 2015b. Multivariable analysis of micro shearing process customized for progressive forming of micro-parts. International Journal of Mechanical Sciences 93, 191-203.
Mori, K.I., Abe, Y., Suzui, Y., 2010. Improvement of stretch flangeability of ultra high strength steel sheet by smoothing of sheared edge. Journal of Materials Processing Technology 210, 653-659.

Narayanasamy, R., Narayanan, C.S., Padmanabhan, P., Venugopalan, T., 2010. Effect of mechanical and fractographic properties on hole expandability of various automobile steels during hole expansion test. International Journal of Advanced Manufacturing Technology 47, 365-380.

Sato, H., Manabe, K., Ito, K., Wei, D., Jiang, Z., 2015. Development of servo-type micro-hydromechanical deep-drawing apparatus and micro deep-drawing experiments of circular cups. Journal of Materials Processing Technology 224, 233-239.

Soussi, H., Masmoudi, N., Krichen, A., 2016. Analysis of geometrical parameters and occurrence of defects in the hole-flanging process on thin sheet metal. Journal of Materials Processing Technology 234, 228-242.

Thipprakmas, S., Jin, M., Murakawa, M., 2007. Study on flanged shapes in fineblanked-hole flanging process (FB-hole flanging process) using finite element method (FEM). Journal of Materials Processing Technology s 192–193, 128-133.

Thipprakmas, S., Phanitwong, W., 2012. Finite element analysis of flange-forming direction in the hole flanging process. International Journal of Advanced Manufacturing Technology 61, 609-620.

Vollertsen, F., Schulze Niehoff, H., Hu, Z., 2006. State of the art in micro forming. International Journal of Machine Tools and Manufacture 46, 1172-1179.

Wang, J.L., Fu, M.W., Ran, J.Q., 2013. Analysis and avoidance of flow-induced defects in meso-forming process: simulation and experiment. International Journal of Advanced Manufacturing Technology 68, 1551-1564.

Table and Figure Captions

Table 1 Annealing conditions and different grain sizes of the testing material.

Table 2 Tool geometry parameters used in the hole flanging-ironing integrated process.

Fig. 1. Hole-flanging process with and without ironing.

Fig. 2. Microstructures of the testing materials: (a) as-received; (b) 500 °C annealed; (c) 600 °C annealed and (d) 750 °C annealed.

Fig. 3. The strain-stress curves of pure coppers with diverse initial microstructures.

Fig. 4. The unequal-thickness micropart and its dimensions: (a) geometrical dimensions and (b) photo of the deformed part by scanning electron microscope (SEM).

Fig. 5. The experimental die layout and the finished microparts.

Fig. 6. Tool geometrical parameters of the hole flanging-ironing process.

Fig. 7. Load-stroke curves of micro hole flanging-ironing under different grain sizes.

Fig. 8. Forming kinematics of the hole flanging-ironing process.

Fig. 9. Different zones of the fabricated billets.

Fig. 10. Distributions of different zones of the sheared pin under diverse material conditions.

Fig. 11. Comparison of the length and final shape of the fabricated micro-pins.

Fig. 12. Change of surface integrity with grain size.

Fig. 13. Effect of grain size on the geometric dimensions of the flanged part: (a) flange height, and (b) tapering angle between inner and outer surfaces.

Fig. 14. Schematic illustration of the free surface roughening and the lubricated effect on the tapering angle.

Fig. 15. Effect of grain size on the diameters of the finished micropart.

Fig. 16. Microstructure evolution in micro-scale shearing process with different initial grain sizes: (a) 14.5; (b) 36.9; (c) 44.0 and (d) 67.7 μm.

Fig. 17. Microstructural evolution in the integrated micro-scale hole flanging-ironing process.